DOI: 10.31401/WS.2022.proc.06

Critical Frequency of Ionospheric F1 and F2 Layers and Comparison with Solar Flares Observed in the 24th Solar Cycle

Kilcik A., Tirnakci M.

Department of Space Science and Technologies, Akdeniz University Faculty of Science, 07058, Antalya, Turkey

Abstract

In this study, the number of X-ray solar flares (SFs) that observed during the solar cycle 24 (2008-2020) were compared with the ionospheric F_1 and F_2 layers critical frequencies (f_0F_1, f_0F_2). The temporal variations, cross-correlation and hysteresis analyses were applied. The monthly median ionospheric critical frequency values are taken from the UK Solar System Data Center-Sodankyla (67°N,26°E), while the X-ray Solar flare data are taken from the Laboratory for Experimental Astrophysics (LEA). We found following results; in the temporal variation analysis, especially the critical frequency of the F_1 layer and the total SF, C and X class SF seems to be quite compatible. The critical frequency of the F_2 layer and the number of total X-Ray solar flares show also good agreement with the number of SFs. Critical frequency of ionospheric F_1 and F_2 layers show meaningful positive correlation with total SF numbers (r=0.38, r=0.59, respectively). It has been observed that the separation between the hysteresis analysis and the path shows different cycles, the critical frequency of the F_1 layer has a wider cycle than the critical frequency of the F_2 layer.

Introduction

The sun is the main energy source of the solar system and emits radiation of all wavelengths intervals of electromagnetic spectrum from gamma to radio. Especially ultraviolet (UV) irradiance in the range of 115-420 nm, in the lower thermosphere, mesosphere and stratosphere have a significant effect on temperature distribution, photochemistry and all momentum balance (Ozguc et al., 2008). Ionosphere; since it occurs in the lower thermosphere, mesosphere and exosphere layers, and the energy coming from the Sun directly affects the ionospheric layers. Particularly, extreme UV (EUV) causes photoionization, and thus changes the electron density of the ionospheric layers (Ikubanni et al., 2013). The ionosphere divided into three layers as D, E and F according to the ionized components in these layers. Also, radiation coming from the sun split the F layer into two sublayers as F_1 and F_2. In the F1 layer NO^+ and O_2^+ are the principal ionized component and the main ionization source is EUV. Height of this layer varies with solar zenith angle, geomagnetic activity and seasonal variations. It is more evident primarily in the summer and is not usually observed at night and winter. The dominant charge transporter in the F2 layer is O^+. The main source of ionization in this layer is also photoionization process due to solar EUV radiation. This layer has highly variable nature and the most important property of this layer is existence for 24 hours under all solar-terrestrial conditions, which means it is a very important layer for radio communications. The F layers have a certain maximum frequency at which they can reflect back the radio waves sent from the Earth. This maximum frequency is called the ionospheric critical frequency.
In addition to EUV, the X-ray flux coming from the Sun with the solar flare causes an additional photoionization of all neutral components in the lower ionosphere, including excess elements in the atmosphere, e.g., oxygen, nitrogen (Whitten and Poppoff, 1965). It is known that amount of solar EUV and X-ray fluxes are dependent on solar activity (Ozguc et al., 1998).

Solar flares are sudden increases in brightness observed on the solar surface and are caused by the release of magnetic energy around sunspots. During SF, energy is emitted from the Sun at all wavelengths, but most of them fall outside the visible region as these are quite

high energies. They classified in two classification schemas depend on their observation as, Hα and X-ray classifications. Hα classification is based on the size of the flare region and the intensity of the brightness. Depending on the peak flux in X-ray wavelength interval (1-8 Å) they also classified in five different classes as A, B, C, M and X.
Sunspot number, which is the most obvious indicator of solar activity, was compared with X-ray SF by Hathaway (2015). The M and X class SF numbers seen in the 1.0–8.0 Å band tend to follow the sunspot number and they found that there is a trend for more SF to emergence in the descending phase of the sunspot cycle. Kilcik et al. (2011a) suggested that the maximum CME speed index (MCMESI) can be considered as an indicator of solar activity and geomagnetic activity. Again, Kilcik et al. (2020) found that the MCMESI showed a significant positive correlation with X-ray flare numbers and both data sets also had similar periodic behaviors.

In this study, solar X-ray flare numbers compared with foF1 and foF2 during the solar cycle 24. We describe data and methods used are given in Section 2, analysis and results are given in Section 3, and the discussion and conclusions are presented in Section 4.

Data and Methods

The ionospheric monthly median critical frequency values (f_0F_1 and f_0F_2) are taken from the UK Solar System Data Centre (https://www.ukssdc.ac.uk/wdcc1/iono_menu.html). We used Sodankylä (67°N, 26°E) station data due to the existence of complete f_0F_1 and f_0F_2 data during the solar cycle 24. The monthly median values exist for each hour in the data source and we chose the data for 14:00 local time (LT) for each month. Especially the F_1 layer is highly dependent on the seasonal variations and solar zenith angle there were lots of gaps in f_0F_1 data during the winter months for the investigated time period, while f_0F_2 data exists in all cases. Therefore, we used f_0F_1 data that have monthly median values during a year and used in correlation analysis. The f_0F_2 data are used directly in the study for the investigated time period.
Solar X-ray flare data are taken for each day from Laboratory for Experimental Astrophysics (LEA) (http://www.ioffe.ru/LEA/Solar/) for classes C, M, and X. Then, the number of daily X-ray flares and their monthly mean values were produced for above classes.
As a first step, to remove the small fluctuations and reveal the general trend the 11-step running average smoothing method were applied to all data sets. Thus, the temporal variation plots were produced (see Figure 1). To obtain the relationship between the number of X-Ray solar flares (total and separate classes) and ionospheric critical frequencies (f_0F_1 and f_0F_2) the cross-correlation analysis methods were applied directly to the monthly values. To measure the error levels of obtained correlation coefficients the Fisher test statistics were performed. This test gives us the upper and lower limits of obtained correlation coefficient with 95% confidence.
Finally, we plotted hysteresis behaviors of the number of X-Ray solar flares and the ionospheric critical frequencies. For this analysis the yearly average values were used. If there is a temporal offset between compared two parameters, then the scatterplot will exhibit a loop like structure and this kind scatterplot called hysteresis plot in the literature (Bachmann et al., 2004). The width of loops describes the amount of time delay and the direction of rotation show the which parameter following the other (Ozguc et al., 2016).

Analysis and Results

As a result of our analysis, temporal variation plots are produced as shown in Figure 1. According to this, f_0F_2 data show multiple peak structure like solar activity, while the f_0F_1 data do not.
There is a small peak in all classes flare number data around 2017 and f_0F_1 temporal profile show similar peak with about five-month delay.

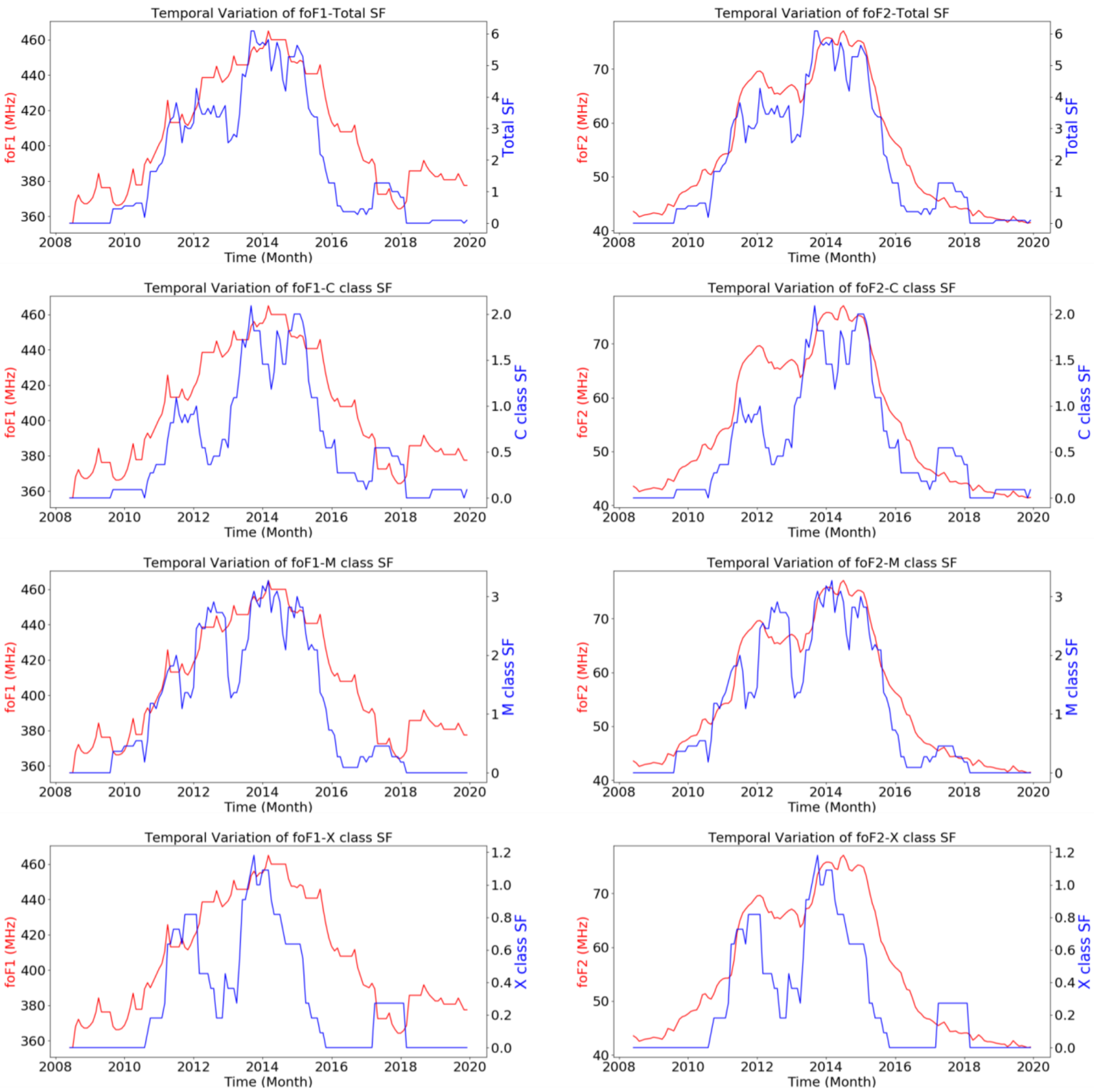

Figure 1. Temporal variation of all parameters used in this study.

Figure 2. shows the cross correlations of f_0F_1 - f_0F_2 and solar X-ray flares number. The results of these plots are also presented in Table 1.

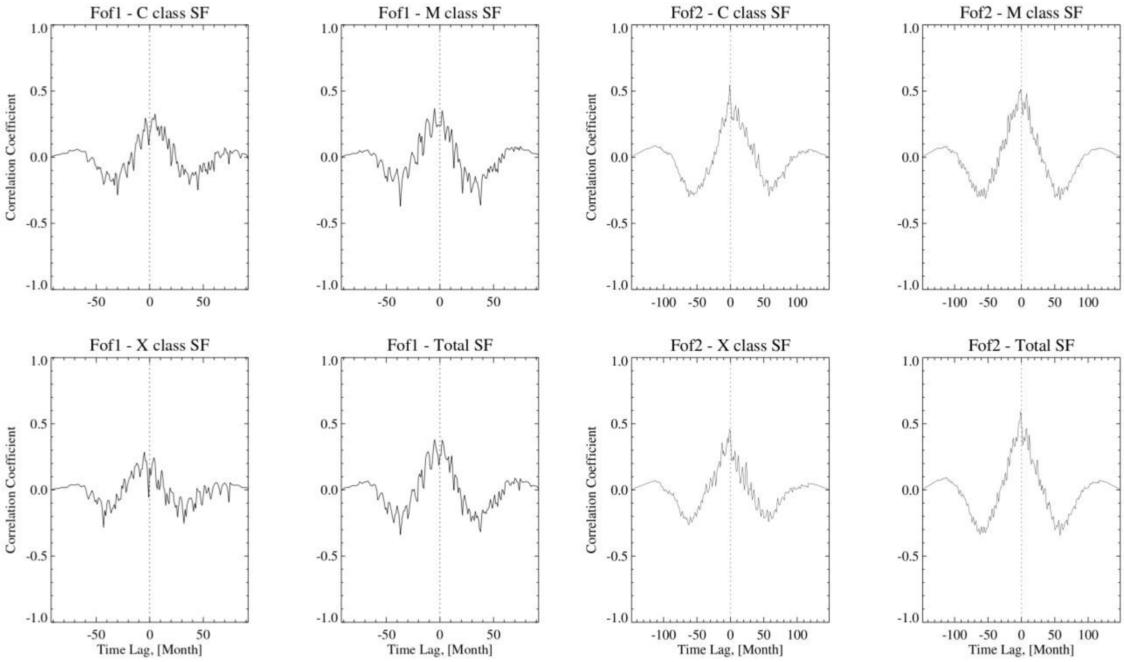

Figure 2. Cross-correlation analysis results between f_0F_1/f_0F_2 and the number of all solar X-ray flares.

Table 1. Cross-correlation coefficients and their corresponding time delays

	f_0F_1- Total SF	**f_0F_1-C Class SF**	**f_0F_1-M Class SF**	**f_0F_1-X Class SF**	**f_0F_2- Total SF**	**f_0F_2-C Class SF**	**f_0F_2-M Class SF**	**f_0F_2-X Class SF**
Cross Correlation Coefficient	0. 38±0.19	0.33±0.19	0.37±0.19	0.29±0.2	0.59±0.12	0.54±0.12	0.51±0.13	0.46±0.14
Time Delay (Month)	-5	5	-5	-5	-1	-1	-1	-1

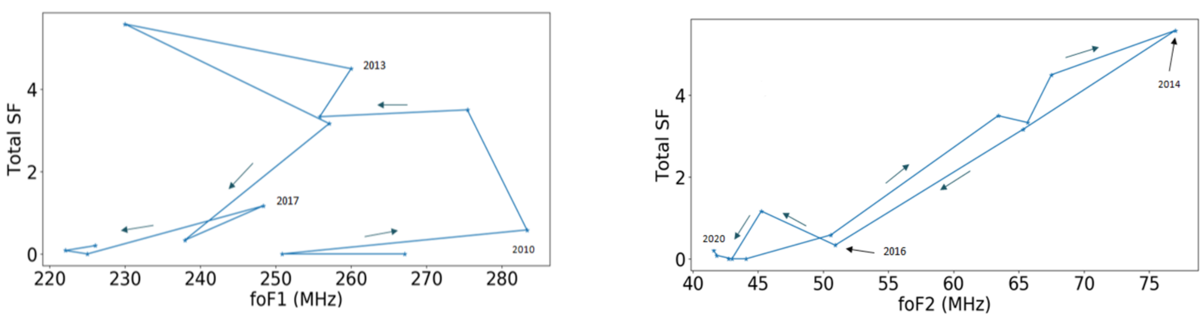

Figure3. Scatter plots showing the hysteresis phenomenon between f_0F_1/ f_0F_2 and the number of total X-Ray flares.

Figure 3 shows the hysteresis analysis results between the number of total X-ray flares and critical frequencies. From this figure we achieved following results; i) In general, the hysteresis cycle exhibit almost regular clockwise circulation for f_0F_2. This result indicates that f_0F_2 behind the X-Ray solar flares. The ascending phase shows higher track than the descending phase and this confirm above result. The only hysteresis behavior appears around the end of declining phase, ii) for the f_0F_1 the situation is quite different; the hysteresis cycles exhibit counterclockwise circulation and very wide pattern. This means there is time lag between two parameters and the hysteresis patterns appear around minima.

Discussion and Conclusion

In this study, monthly median f_0F_1, f_0F_2 and the number of solar X-ray flares (C, M, and X classes) were investigated during the solar cycle 24. We obtained the following results:

1. f_0F_2 and all X-Ray SF classes show similar temporal behaviors with their double/multiple peak structures, while the f_0F_1 has a single peak structure.
2. In general, the number of total SF show higher correlation compared to separate classes and the f_0F_2 data has also stronger correlation than f_0F_1.
3. f_0F_1 shows more hysteresis behavior compared to f_0F_2
4. The hysteresis behaviors show opposite circulations; f_0F_2 has clockwise circulation, while f_0F_1 has counterclockwise.
5. In both cases the hysteresis behaviors appear mainly around the cycle's minima.

Active events such as solar flares and CMEs occur around large/complex active regions (Kilcik et al. 2011b). It is observed that solar cycle 24 had double peak structures. Thus, we may expect double peak structure for the temporal variation of ionospheric critical frequencies. Yiğit et al (2018) argued that f_0F_2 and hence the F_2 region is more sensitive to active sun (solar flares, CMEs), while f_0F_1 and hence the F_1 region is sensitive to quiet sun. Our findings in Figure 1 confirm their results. Kilcik et al (2018) found that during solar cycle 24 both critical frequencies were lower compared to cycle 23 (see Fig. 2 in their paper). This result indicates that the amplitude of the ionospheric frequencies (f_0F_1 and f_0F_2) is strongly correlated with the amplitude of solar activity. In addition, Burns et al (2007) emphasized that the ionospheric F_2 layer is more sensitive to geomagnetic activity and CMEs. Here we found that the number of X-ray flare show higher correlation with f_0F_2 compared to f_0F_1. Thus, we may confirm their results for solar cycle 24.

Solar flares and CMEs both are strong active events and some of them are related. High-latitude CMEs are closely associated with polar crown filaments, while low-latitude CMEs are mainly related to sunspots (Gopalswamy et al., 2010). Kilcik et al (2018) performed correlation analysis between MCMESI and f_0F_1 - f_0F_2 and found meaningful correlations (r=0.39, r=0.68, respectively) for Solar cycle 24. In this study, we obtained that the number of total solar X-Ray flares show almost the same level correlation (r=0.38, r=0.59, respectively). This result may confirm the relation between CMEs and X-ray solar flares and further we may speculate that CMEs are more effective for ionospheric critical frequencies.

In the hysteresis analysis, a large loop indicates time delay, while clockwise loops indicate that the variable on the x-axis lags behind the variable on the y-axis (Özgüç et al., 2016). Here we found 5-month time delay between f_0F_1 and solar ray flare (see Table 1) and counter-clockwise loop. For the f_0F_2 contrary results were obtained for rotation and much less time delay. The 1-month delay may explain the narrow cycle in Figure 3 and f_0F_2 follow behind the solar X-ray flares. Note that all hysteresis behaviors appear around the cycle minima. Özgüç et al. (2012) concluded that hysteresis may occur due to the fact that magnetic fields of different scales make different contributions to the total magnetic flux at various stages of the cycle. Here we confirm their results for solar cycle 24 and further suggest that the hysteresis behavior observed around minima may explained by using their argument.

References

Bachmann, K. T., Maymani, H., Nautiyal, K., & Te Velde, V. (2004). An analysis of solar-cycle temporal relationships among activity indicators. *Advances in Space Research*, *34*(2), 274-281.

Burns, A.G, Solomon, S. C., Wang, W., and Killeen. T. L. (2007). The ionospheric and thermospheric response to CMEs: Challenges and successes, J. Atmos. Sol.-Terr. Phys., 69, 77–85.

Gopalswamy, N., Akiyama, S., Yashiro, S., & Makela, P. (2010). in Magnetic Coupling between the Interior and Atmosphere of the Sun, ed. S. Hasan & R. J. Rutten (Berlin, Heidelberg: Springer Berlin Heidelberg), 289–307

Hathaway, David H. (2015). "The solar cycle." *Living reviews in solar physics* 12.1,1-87.

Ikubanni, S. O., Adebesin, B. O., Adebiyi, S. J., & Adeniyi, J. O. (2013). Relationship between F2 layer critical frequency and solar activity indices during different solar epochs. *94.20. dj; 96.60. qd*.

Kilcik, A., Yurchyshyn, V. B., Abramenko, V., Goode, P. R., Gopalswamy, N., Ozguc, A., & Rozelot, J. P. (2011a). Maximum coronal mass ejection speed as an indicator of solar and geomagnetic activities. *The Astrophysical Journal*, *727*(1), 44.

Kilcik, A., Yurchyshyn, V. B., Abramenko, V., Goode, P., Ozguc, A., Rozelot, J. P., & Cao, W. (2011b). Time distribution of large and small sunspot groups over four solar cycles, The Astrophysical Journal, 730, 30–37.

Kilcik, A., Ozguc, A., Yiğit, E., Yurchyshyn, V., & Donmez, B. (2018). Signature of a possible relationship between the maximum CME speed index and the critical frequencies of the F1 and F2 ionospheric layers: Data analysis for a mid-latitude ionospheric station during the solar cycles 23 and 24. J. Atmos. Sol.-Terr. Phys., *171*, 131-136

Kilcik, A., Chowdhury, P., Sarp, V., Yurchyshyn, V., Donmez, B., Rozelot, J. P., & Ozguc, A. (2020). Temporal and periodic variation of the MCMESI for the last two solar cycles; Comparison with the number of different class X-ray solar flares. *Sol. Phys.*, *295*(11), 1-17.

Özgüç, A., Tulunay, Y., ATAÇ, T. (1998). Examination of the solar cycle variation of foF2 by using solar flare index for the cycle 21. *Advances in Space Research*, 22.1: 139-142.

Özgüç, A., Ataç, T. and Pektaş, R. (2008). "Examination of the solar cycle variation of foF2 for cycles 22 and 23." J. Atmos. Sol.-Terr. Phys., 70.2-4, 268-276.

Özgüç, A., Kilcik, A. and Rozelot, J. P. (2012). "Effects of Hysteresis Between Maximum CME Speed Index and Typical Solar Activity Indicators During Cycle 23." *Sol. Phys.*, 281.2, 839-846.

Özgüç, A., Kilcik, A., Georgieva, K., & Kirov, B. (2016). Temporal Offsets Between Maximum CME Speed Index and Solar, Geomagnetic, and Interplanetary Indicators During Solar Cycle 23 and the Ascending Phase of Cycle 24. *Sol. Phys.*, *291*(5), 1533-1546.

Whitten R. C., Poppoff I. G. (1965). Physics of the Lower Ionosphere, Prentice- Hall, Inc. Englewood Cliffs, N. J.

Yiğit, E., Kilcik, A., Elias, A. G., Dönmez, B., Ozguc, A., Yurchshyn, V., & Rozelot, J. P. (2018). Critical frequencies of the ionospheric F_1 and F_2 layers during the last four solar cycles: Sunspot group type dependencies. J. Atmos. Sol.-Terr. Phys., *171*, 157-163.